Research Square

Preprints are preliminary reports that have not undergone peer review.
They should not be considered conclusive, used to inform clinical practice,
or referenced by the media as validated information.

Quantifying the Protective Role of the Sundarbans Mangroves Against Cyclones Using Landsat-Derived NDVI and EVI (2007–2024)

Tania Sultana

tania.tona19@gmail.com

Khulna University

Kazi Sajirul Kadir Apon

Jahangirnagar University

Research Article

Keywords: Sundarbans, NDVI, EVI, Cyclone Impact, Mangrove Protection, Remote Sensing, Coastal Resilience, Bangladesh

Posted Date: March 24th, 2026

DOI: https://doi.org/10.21203/rs.3.rs-9042474/v1

License: This work is licensed under a Creative Commons Attribution 4.0 International License.
Read Full License

Additional Declarations: No competing interests reported.

Version of Record: A version of this preprint was published at Journal of Coastal Conservation on August 4th, 2026. See the published version at https://doi.org/10.1007/s11852-026-01262-x.

Quantifying the Protective Role of the Sundarbans Mangroves Against Cyclones Using Landsat-Derived NDVI and EVI (2007–2024)

Tania Sultana[1]*, Kazi Sajirul Kadir Apon[2]

[1] Department of Development Studies, Khulna University, Khulna 9208, Bangladesh
Present address: Itagacha, Bakal, Satkhira Sadar, Satkhira 9400, Bangladesh
Email: tania.tona19@gmail.com

[2] Department of Geography and Environment, Jahangirnagar University, Savar, Dhaka, Bangladesh
Present address: Khorki, Jashore Sadar, Jashore 7400, Bangladesh
Email: sajirulk@gmail.com

Corresponding Author

Tania Sultana
Department of Development Studies, Khulna University, Khulna 9208, Bangladesh
Present address: Itagacha, Bakal, Satkhira Sadar, Satkhira 9400, Bangladesh
Email: tania.tona19@gmail.com

1. Abstract:

The Sundarbans, the largest mangrove forest in the world, acts as a major natural defense against cyclones along the coast of Bangladesh. This paper examines the relationship between vegetation health (measured by the Normalized Difference Vegetation Index, NDVI, and the Enhanced Vegetation Index, EVI) and cyclone-induced deaths and housing losses from 2007 to 2024. Remote sensing data from Landsat, cyclone impact data from the Bangladesh Bureau of Statistics (BBS) and EM-DAT, and spatial GIS were integrated to measure vegetation change and cyclone impact in Sundarban-protected and unprotected coastal districts. Findings indicate a minor shrinkage in thick vegetation (86 percent in 2007 to 85 percent in 2024) and growth in water bodies, which are evidence of erosion and storm activities. Regression analysis showed that EVI exhibited strong negative relationships with the death rate (**β** = -0.888, p = 0.018) and the house damage rate (**β** = -0.962, p = 0.002) in protected areas, supporting the argument that healthier vegetation reduces cyclone losses. Similar, but weaker relations were found in NDVI.The results point to the vitality of the Sundarbans in protecting the coastal area and the necessity of continuous vegetation control and mangrove restoration to enhance long-term cyclone resistance in Bangladesh.

Keywords: Sundarbans, NDVI, EVI, Cyclone Impact, Mangrove Protection, Remote Sensing, Coastal Resilience, Bangladesh.

2. Introduction:

Bangladesh is a densely populated nation with low-lying coastline and a geographical position in the Bay of Bengal, which makes it vulnerable to cyclones and one of the most vulnerable countries on the planet. The coastal lands are frequently hit by tropical cyclones which result in high loss of lives, property damages and loss of livelihood (Arif et al., 2023; Mamun et al., 2025). The Sundarbans, the largest mangrove forest in the world, is important as a natural protective feature that mitigates the effects of storm surges and wind velocity on nearby settlements (Mancheno et al., 2025). The rising intensity of cyclones caused by climate change, along with enhanced land use change and forest degradation, has raised questions regarding the long-term sustainability of the natural defence mechanism (Islam et al., 2024). Recent reports indicate a significant shift in vegetation and land cover in the Sundarbans, accompanied by a slowing decline in dense forest cover and increased fragmentation (Zhang et al., 2023; Hossain et al., 2024; Roy et al., 2025). These ecological changes have an implication on the capacity of the forest to respond to disaster risks, less canopy density and deterioration can result in loss of buffering capacity against cyclones. Despite such studies having been conducted to understand vegetation changes and mapping cyclone exposure, not many studies have quantitatively determined the relationship between vegetation indices, including NDVI and EVI, and cyclone-induced damages in the form of deaths and destruction of houses (Ali et al., 2025). Furthermore, though the protective value of mangroves is widely known, there has been little empirical research that can compare the areas under Sundarban protection and the uncovered coastal regions of Bangladesh (Siddique et al., 2024). In light of this inconsistency, the present study examines the relationship between vegetation cover, cyclone intensity, and socioeconomic losses, utilizing 2 years of cyclone data from 2007 to 2024. Particularly, it discusses the association of the differences in death rates, as well as house damage rates between Sundarban-protected and unprotected districts with the differences in vegetation indices (NDVI, EVI). The data analysis employs Pearson correlations and regression models to identify the primary contributors to cyclone damage, as well as to spatially map cyclone tracks and vegetation patterns using GIS and remote sensing.

The study is relevant to both the appropriate scientific knowledge and policy-making. It develops the scientific discussion of nature-based solutions by testing the disaster-mitigating effects of mangrove ecosystems under various changing environmental conditions (Mancheno et al., 2025).

On the policy level, the results can be used in the management of coastal disasters and where forest conservation and restoration can be most effective at minimizing cyclone risks. Ultimately, this research paper is relevant to the broader climate resilience agenda because it establishes a connection between ecological processes in the Sundarbans and the socio-economic vulnerability of the Bangladesh coast.

3. Materials and Methods:

3.1. Study Area:

The study was conducted in the Sundarbans, which is the largest continuous mangrove forest in the world, and is found in the southwestern coastal area of Bangladesh. (**Fig. 1**) indicates the geographical location of the Sundarbans and the coastal districts. The Bangladeshi Sundarbans is geographically positioned between 21°31' and 22°30'N latitude and 89°00' and 89°55'E longitude, occupying an area of approximately 6,017 km², which is close to 62 percent of the entire Sundarbans ecosystem (Iftekhar et al., 2015). An intricate system of rivers, tidal creeks and mudflats cuts across the forest, making it a dynamic estuarine ecosystem at the meeting point of the Ganges, Brahmaputra and the Meghna rivers. The Sundarbans is also considered to be a UNESCO World Heritage Site globally and is a critical ecological unit in defending the populated coastal districts of Khulna, Satkhira and Bagerhat in the Bay of Bengal against cyclonic storms and tidal waves (Das & Vincent, 2009). The mangrove cover serves as a natural bio-shield by reducing the speed of the wind, breaking the energy of the waves and lowering the height and intensity of storm surges before they can reach the inland human settlements. The climatic conditions of the area include tropical monsoonal weather, more than 1,800 mm of precipitation each year, elevated humidity, and the temperature averages 12°C and 35°C each month (Shahid & Behrawan, 2008). The Sundarbans have traditionally borne the brunt of several disastrous cyclones, including Sidr (2007), Aila (2009), Amphan (2020), Yaas (2021), and Remal (2024), which typically occur in the pre-monsoon (April-May) and post-monsoon (October-November) seasons. The communities surrounding the Sundarbans rely extensively on the Sundarbans resources in terms of fuelwood, fish, honey, and timber. Still, they are also highly vulnerable to disasters due to their location close to cyclone landfall areas. The surrounding districts, such as Khulna, Satkhira, and Bagerhat, have population densities of over 800 persons per square

kilometre (BBS, 2022), with many households residing in kutcha houses that are quickly constructed and most of which are susceptible to destruction by cyclones (Paul & Routray, 2011). So, the Sundarbans is not only a life-bearing ecosystem, but also a disaster-insuring barrier to millions of people. The analysis of vegetation density variations using NDVI/EVI and their correlation with cyclone-induced damages provides essential information on the role of mangroves in enhancing resilience in climate-sensitive coastal Bangladesh.

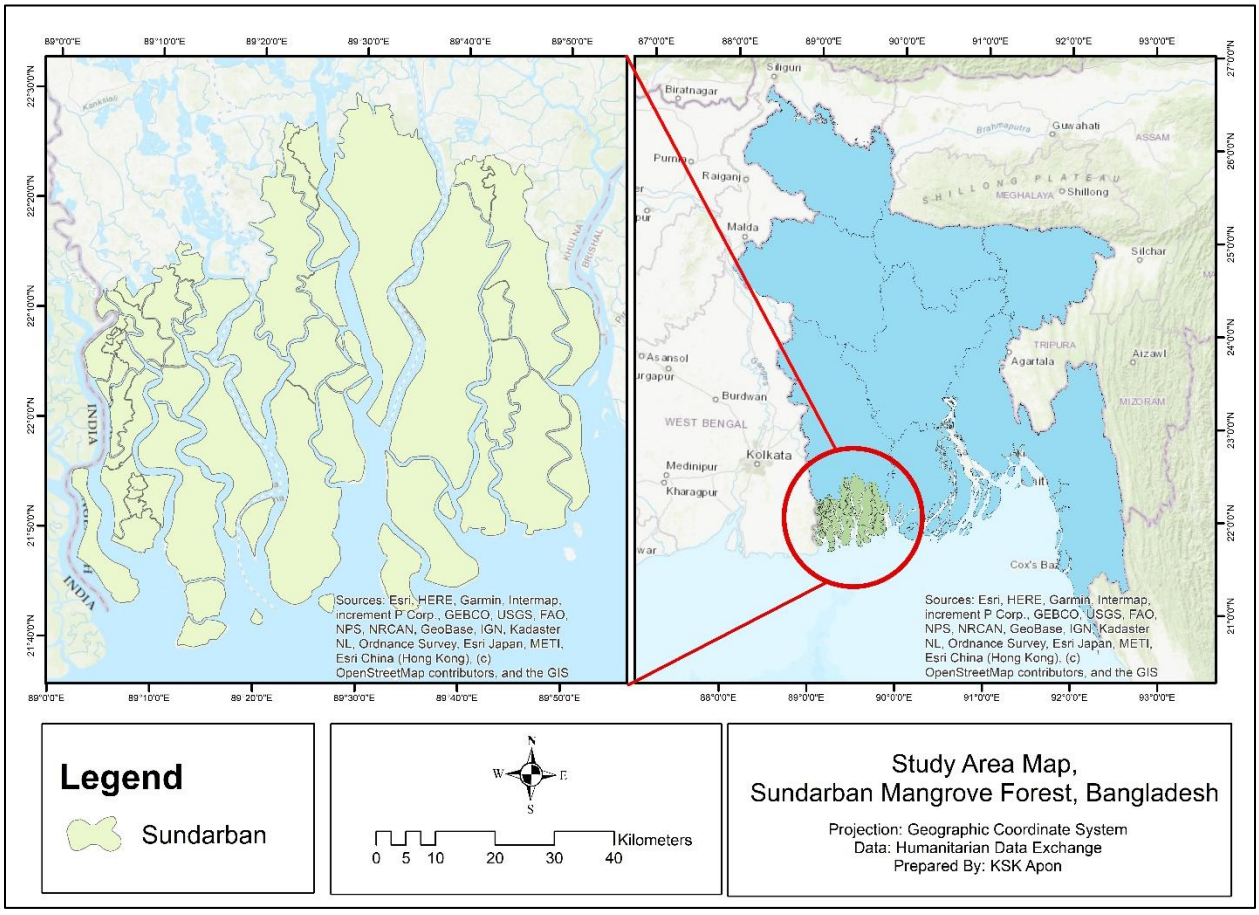


Fig. 1 Study Area Map

2.2. Data Sources:

In this research, remote sensing, socio-economic, and disaster impact data were combined to determine how vegetation activities correlate with cyclone-related damages in the Sundarbans region. Landsat satellite data from 2007, 2009, 2019, 2020, 2021, and 2024 were used to derive vegetation data, which matched the years of major cyclones. These pictures were acquired on the United States Geological Survey (USGS) platform Earth Explorer with a spatial resolution of 30

meters. To measure vegetation density, NDVI and EVI indices were calculated, and reclassification was done to classify water, sparse, moderate, and dense cover types. The data concerning cyclones, such as the speed of the wind, the height of the surge, the date and time of landing, number of deaths, and the damage to properties, were acquired via the Bangladesh Bureau of Statistics (BBS), Ministry of Disaster Management and Relief (MoDMR), and international disaster databases including EM-DAT (Emergency Events Database). Data on population and households were obtained based on the Population and Housing Census of Bangladesh (2011 and 2022), and estimates of households were obtained based on the average household size offered by BBS. These data were crucial for computing the rates of death (per 100,000 population) and house damage rates (per 100,000 households). The data on cyclone tracks and space were obtained from the International Best Track Archive for Climate Stewardship (IBTrACS), which is maintained by NOAA, and were subjected to GIS-based spatial analysis. Peer-reviewed articles and government reports were used to gather additional contextual data about socio-economic vulnerability and disaster response (**Table 1)**.

Table 1: Data Sources

Data Type	Source	Years Used	Purpose
Landsat Satellite Imagery	USGS Earth Explorer (Landsat 5 TM, 8/9 OLI)	2007, 2009, 2019, 2020, 2021, 2024	NDVI and EVI calculation, vegetation classification (water, sparse, moderate, dense)
Cyclone Characteristics	Ministry of Disaster Management & Relief (MoDMR), BBS, EM-DAT	2007–2024 (major cyclones)	Wind speed, surge height, death toll, house damage statistics

Population Data	Bangladesh Bureau of Statistics (Population and Housing Census 2011, 2022)	2007–2024 (estimates)	District-level population and household size for death/damage rate calculation
Household Size	BBS Household Survey	2011, 2022	Used to estimate number of households from population data
Cyclone Track Data	IBTrACS (NOAA)	2007,2009,2019,2021,2024, and 2024	Mapping cyclone tracks, kernel density, and spatial analysis in ArcGIS
Secondary Literature	Peer-reviewed journals, reports	2007–2025	Contextual data on Sundarbans ecology, cyclone impacts, and vulnerability

3.2. Image preprocessing:

To ensure the quality and reliability of the data used, pre-processing of satellite imagery was performed before calculating the vegetation indices. Data from 2007, 2009, 2019, 2020, 2021, and 2024, as observed in Landsat imagery (Landsat 5 TM and 8/9 OLI), were downloaded from the USGS Earth Explorer platform in Level-1 GeoTIFF format. The following steps were used:

3.2.1. Radiometric and Atmospheric Correction:

Digital Number (DN) values were initially transformed to Top-of-Atmosphere (TOA) reflectance using radiometric calibration parameters included in the metadata. Then, the Dark Object Subtraction (DOS) method was employed to perform atmospheric correction and mitigate the effects of atmospheric scattering and absorption (Chavez, 1996).

3.2.2. Geometric Correction and Projection:

All images were reprojected to a single standard coordinate system, WGS 1984 UTM Zone 46N, to ensure spatial coherence. Visual checks of images were conducted to match them with reference data.

3.2.3. Cloud and Shadow Masking:

Scenes were carefully chosen to minimize cloud contamination. In the case of its existence, the Fmask algorithm, which is part of Landsat QA bands, was used to mask clouds and shadows (Zhu and Woodcock, 2012).

3.3. Vegetation Indices:

To determine the vegetation condition in the Sundarbans, two spectral indices were calculated: the Normalized Difference Vegetation Index (NDVI) and the Enhanced Vegetation Index (EVI). The indices have been widely applied in tracking vegetation greenness, canopy density, and health in tropical ecosystems. The standard formula was used to calculate NDVI (Rouse et al., 1974):

$$NDVI = \frac{(NIR - RED)}{(NIR + RED)}$$

In which NIR denotes the near-infrared band (Band 4 in the case of Landsat 5 TM/7 ETM+, Band 5 in the case of Landsat 8/9 OLI), and RED denotes the red band (Band 3 in the case of TM/ETM+, Band 4 in the case of OLI). The values of the NDVI range from -1 to +1, with higher values indicating an increase in vegetation density. EVI was also calculated to complement the NDVI

because it minimizes atmospheric effects and it is more responsive to canopy structural changes (Huete et al., 2002). The EVI formula is:

$$EVI = G \times \frac{(NIR - RED)}{(NIR + C_1 \times RED - C_2 \times BLUE + L)}$$

where NIR, RED, and BLUE correspond to the respective Landsat bands, $L = 1$ is the canopy background adjustment, $C_1 = 6$, $C_2 = 7.5$ are aerosol resistance coefficients, and $G = 2.5$ is the gain factor.

NDVI and EVI images were created each year of analysis (2007, 2009, 2019, 2020, 2021, and 2024) and further reclassified into four vegetation density categories using commonly used threshold values in tropical mangrove research (Giri et al., 2015):

- **Water:** NDVI < 0
- **Sparse Vegetation:** NDVI 0.0 – 0.2
- **Moderate Vegetation:** NDVI 0.2 – 0.4
- **Dense Vegetation:** NDVI > 0.4

3.4. Accuracy Assessment:

The reliability of the NDVI-derived maps, classified into land cover, was determined by performing an accuracy analysis in each of the study years. A stratified random sampling technique was used, where reference points were chosen proportionately in the four classes (water, sparse vegetation, moderate vegetation, and dense vegetation). The outputs of the classification were validated against reference data gathered using high-resolution Google Earth images and available land cover data. A confusion matrix (also known as an error matrix) was used to determine the classification accuracy, where errors were measured based on the number of wrongly classified pixels compared to the number of correctly classified pixels (Congalton, 1991). Based on this, several measures were computed as follows:

- Overall Accuracy (OA): The ratio between the correctly classified pixels and the number of reference pixels.

$$OA = \frac{Total\ number\ of\ correctly\ classified\ pixels\ (Diagonal)}{Total\ number\ of\ refernces\ pixel} \times 100$$

- Producer Accuracy (PA): Represents the degree of classification of real-world land cover types.

$$PA = \frac{Number\ of\ correctly\ classified\ pixels\ in\ eachh\ category}{Total\ number\ of\ refernces\ pixel\ in\ that\ category\ (The\ column\ total)} \times 100$$

- User Accuracy (UA): indicates the consistency of the used categories.

$$UA = \frac{Number\ of\ correctly\ classified\ pixels\ in\ eachh\ category}{Total\ number\ of\ refernces\ pixel\ in\ that\ category\ (The\ row\ total)} \times 100$$

- Kappa Coefficient (T): It is a statistical index applied to explain chance agreement, and it is more effective in classifying the accuracy of the evaluation (Congalton and Green, 2009).

$$Kappa\ Coefficient = \frac{(TS \times TCS) - \sum(Column\ total\ \times Row\ total)}{TS^2 - \sum\ (Column\ total - Row\ total)}$$

Where,

TS= Total Sample and

TCS = Total Corrected Sample,

The results of the accuracy were evaluated in accordance with conventional principles, according to which a total accuracy greater than 85% and a Kappa coefficient higher than 0.80 can be deemed satisfactory for land cover classification (Foody, 2002). These steps were taken to ensure that vegetation dynamics based on the classification were robust enough to facilitate correlation and regression later.

3.5. Socio-economic indicators:

Two important socioeconomic markers were created to measure the human and physical costs of the cyclones in the Sundarbans area: Death Rate and House Damage Rate. The variables enabled the comparative approach to the disaster effects in various cyclone years and sites.

3.5.1. **Death Rate Calculation:** The death rate is the number of cyclone fatalities per 100,000 people in each district, or study area. The formula through which it was calculated is:

$$Death\ Rate = \frac{Total\ death}{Total\ Population} \times 100000$$

Where,

- Total Deaths = Number of people who died due to a specific cyclone (sourced from BBS, MoDMR, and EM-DAT).
- Total Population = Population of the affected district(s) at the time of the cyclone, based on BBS census data (2011, 2022) with intercensal growth applied.
- The factor 100,000 is used to express the rate per 100,000 people for easier comparison across years.

3.5.2. **House Damage Rate Calculation:** The house damage rate is the figure that shows the number of entirely and partially damaged houses per 1000 estimated households in each district or area. It was calculated using:

$$Total\ damaged\ houses = \frac{Total\ house\ damaged\ (Fully + Partial)}{Total\ estimated\ households} \times 1000$$

Where,

- Total Damaged Houses = Sum of fully and partially damaged households reported by BBS or MoDMR.
- Estimated Households = Total population divided by average household size (sourced from BBS household data).
- The factor 1000 standardizes the value for comparative analysis.

3.5.3. Sundarban Protected and Unprotected Area Comparison:

To understand the protective role of mangrove forests, all the affected districts were categorized into two groups:

- Protected Zones: Khulna, Satkhira, and Bagerhat (regions that the Sundarbans directly cover).
- Unprotected Zones: Coastal areas where direct protection of mangroves is absent, including Barguna, Patuakhali, Bhola, Pirojpur, and Jhalokathi.

The average death and house damage rates of each group were calculated and compared in each cyclone year to determine whether high vegetation density is associated with lower human and property losses.

The overall methodological framework of the study is presented in (**Fig. 2**), which summarizes the data sources, processing steps, and analytical workflow.

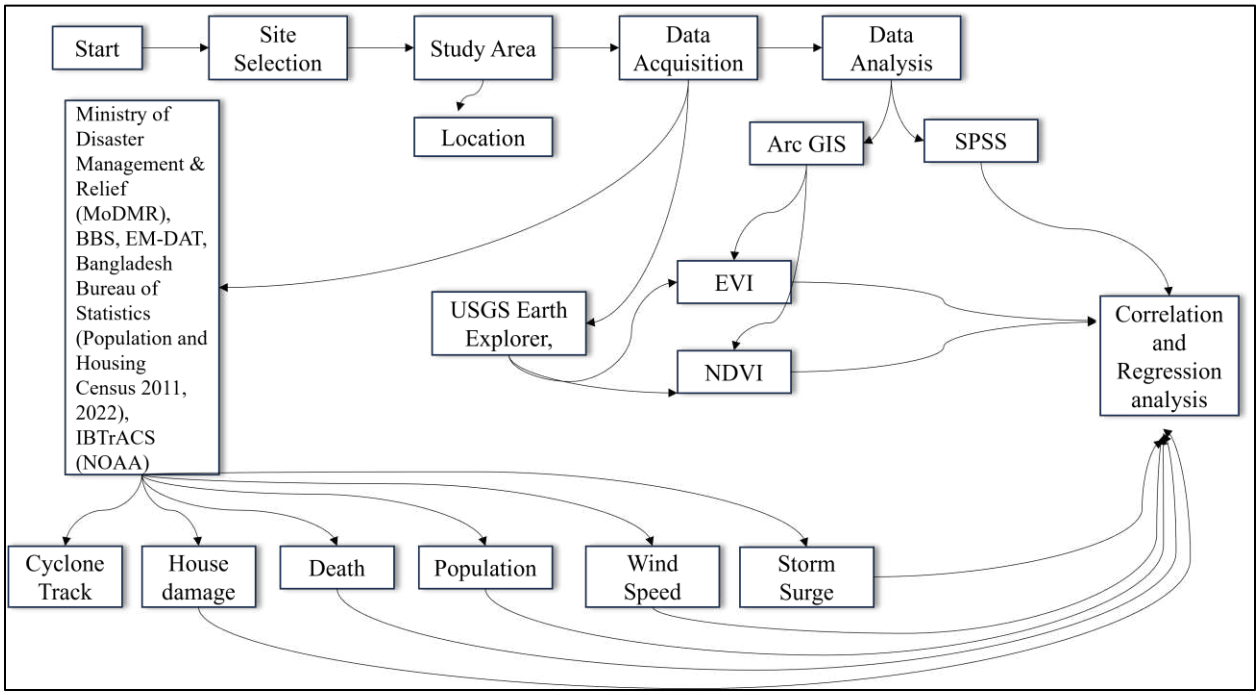


Fig. 2 Methodological Framework

4. Results:

4.1. Vegetation Dynamics in the Sundarbans (2007–2024):

The temporal analysis of NDVI revealed substantial fluctuations in vegetation cover within the Sundarbans during the study period (2007-2024). The mean NDVI values were 0.23 in 2007, 0.21 in 2009, 0.25 in 2019, 0.25 in 2020, 0.27 in 2021, and 0.26 in 2024. Meanwhile, the EVI values ranged from 4.53 in 2007 to 6.73 in 2009, 3.82 in 2019, 3.66 in 2020, 3.71 in 2021, and 4.17 in 2024 (Table 2). (**Fig. 3**) Shows the spatial and temporal variation of NDVI in the Sundarbans between 2007 to 2024. Reclassified NDVI maps revealed that the proportion of dense vegetation varied, which was 86% in 2007, 83% in 2009, 91% in 2019, 78% in 2020, 83% in 2021 and 85% in 2024, while moderate vegetation in 2007 was 9%, 2009 was 12%, 2019 was 3.4%, 2020 was15%, 2021 was 12% and 10 % in 2024. Also, the sparse vegetation of the Sundarban mangrove forest was found to be 3% in 2007, 2009, and 2019, 4% in 2020, 1% in 2024, and water bodies (2, 2, 1.7, 2, 3, and 4 percent) in the years 2007, 2009, 2019, 2020, 2021, and 2024, respectively.

Table 2: Temporal variation in vegetation cover classes and mean vegetation indices (NDVI and EVI) of the Sundarbans from 2007 to 2024

Year	Water	Sparse Vegetation	Moderate Vegetation	Dense Vegetation	Mean NDVI	Mean EVI
2007	2%	3%	9%	86%	0.232885	0.29747
2009	2%	3%	12%	83%	0.213753	0.339401
2019	1.7%	3%	3.4%	91%	0.253881	0.36247
2020	2%	4%	15%	78%	0.250542	0.375626
2021	2%	3%	12%	83%	0.246537	0.385446

2024	3%	1%	10%	85%	0.276599	0.388246

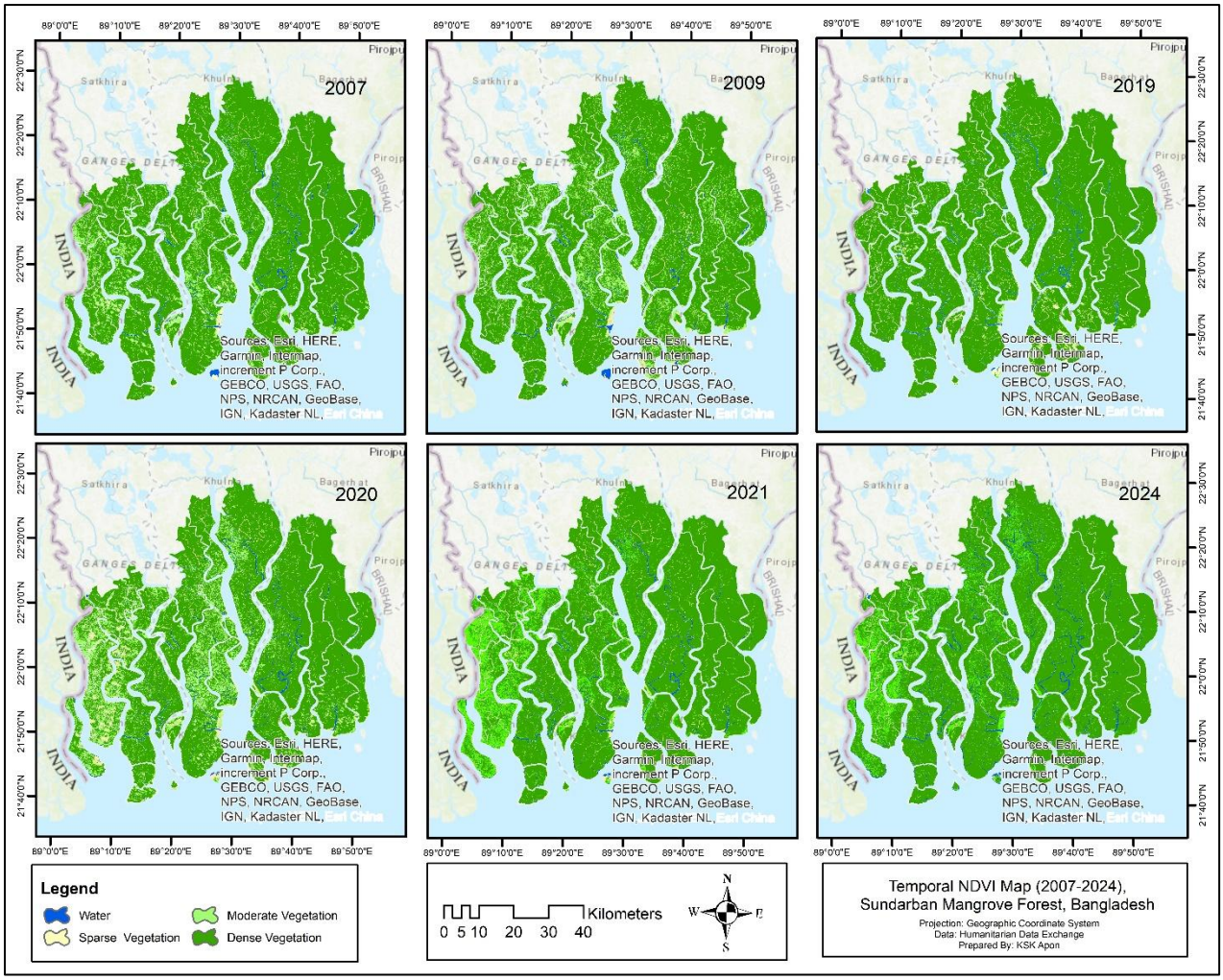


Fig. 3 Temporal NDVI Map (2007-2024), Sundarban Mangrove Forest, Bangladesh

4.2. Temporal Variation of Enhanced Vegetation Index (EVI) in the Sundarbans (2007–2024):

To analyse the vigour and canopy structure of vegetation in the Sundarbans, the Enhanced Vegetation Index (EVI) was studied as a supplement to NDVI from 2007 to 2024. (**Fig. 4**) demonstrates the change of EVI over time during the period of study. The mean EVI scores fluctuated between 0.297 and 0.388, indicating that vegetation health and canopy cover varied over time during the study period. The mean EVI in 2007 was 0.29, in 2009 was 0.33, in 2019 was 0.36, in 2020 was 0.37, in 2021 was 0.38, and in 2024 was 0.38 (Table 2).

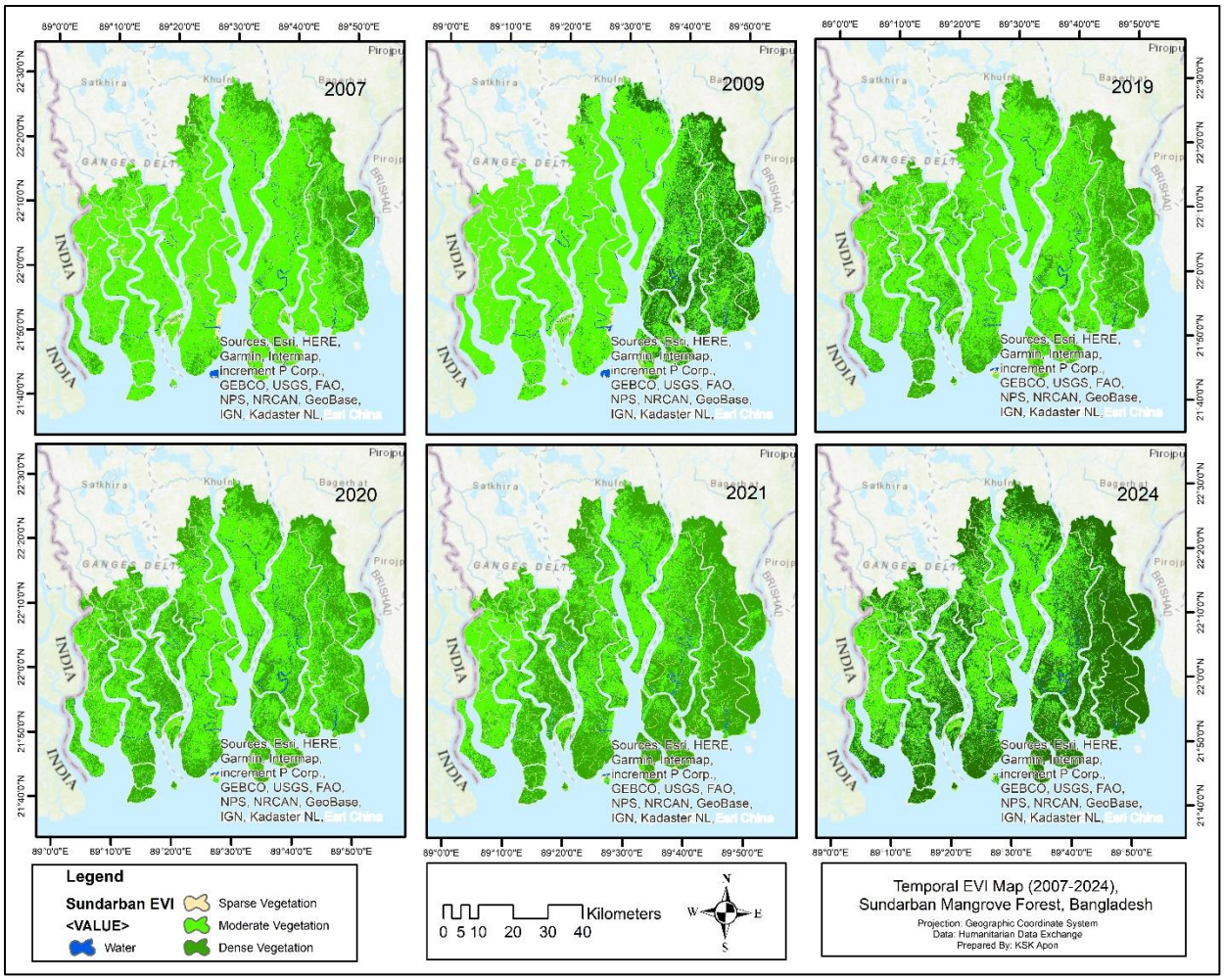


Fig. 4 Temporal EVI Map (2007-2024), Sundarban Mangrove Forest, Bangladesh

4.3. NDVI-Based Vegetation Change Detection (2007–2024):

NDVI-based land-cover change detection analysis of 2007 and 2024 revealed observable spatial changes in the Sundarbans ecosystem. The dense vegetation that covered about 3,588 km^2 of the land in 2007, reduced to 3,551 km^2 in 2024, signifying a slight loss of approximately 37 km^2. The moderate vegetation also increased from 395.7 km^2 to 409.1 km^2, indicating partial regrowth of the forest in the previously degraded areas. The vegetation cover also shrank by a notable 48 per cent to a sparse cover of just 61.9 km^2, while water bodies expanded by approximately 81 km^2, from 63.7 km^2 in 2007 to 144.8 km^2 in 2024 (Table 3).

Table 3: NDVI-Based Vegetation Change Detection Transition Matrix (2007–2024)

2007 → 2024	**Water (2024)**	**Sparse Vegetation (2024)**	**Moderate Vegetation (2024)**	**Dense Vegetation (2024)**	**Total (2007)**
Water (2007)	50.00	5.00	4.00	4.76	**63.76**
Sparse Vegetation (2007)	25.00	40.00	30.00	23.92	**118.92**
Moderate Vegetation (2007)	30.00	5.00	300.00	60.71	**395.71**
Dense Vegetation (2007)	39.80	11.90	75.09	3461.51	**3588.30**
Total (2024)	**144.80**	**61.90**	**409.09**	**3551.10**	**4166.90**

4.4. Comparison of Cyclone-Induced Death and Housing Damage Between Sundarban-Protected and Unprotected Areas:

The comparison of cyclone effects in Sundarban-covered and uncovered districts reveals clear differences in the death rate and house damage rate over time. The comparison of cyclone-induced death rates between protected and unprotected areas is shown in (**Fig. 5)**, while the corresponding house damage rates are illustrated in (**Fig. 6)**. During Cyclone Sidr (2007), the rate of deaths in Sundarban-protected districts (Khulna, Satkhira, and Bagerhat) was approximately 113.10 deaths per 100,000 people. Whereas, it was significantly higher in the unprotected districts at 249.41 deaths per 100,000 people. On the same note, the rate of house damage was significantly higher in the unprotected areas (4,995.04 per 1000 households) than in

the protected areas (2,265.08 per 1000 households), meaning the Sundarbans was a very significant shield against cyclone destruction. The number of casualties (deaths) in the areas where the cyclone protection was in place was 8.25 per 100,000 people in the case of Cyclone Aila (2009), which is somewhat lower than the 10.55 per 100,000 in the uncoded districts. The rate of damage to houses followed a similar trend, with 1,306.37 and 1,669.98 per 1000 households damaged in the protected and unprotected areas, respectively. In the case of Cyclone Fani (2019), the mortality rates were low in both protected and unprotected areas, at 2.04 per 100,000 and 1.91 per 100,000, respectively. The rate of house damage was quite comparable between the two at 48.45 on 1000 in the areas where the house was secured by Sundarban and 45.23 on 1000 in areas where the house was not secured. In Cyclone Amphan (2020), the death rates were close to the safe (1.72 per 100,000) and the unsafe (1.54 per 100,000) districts. There was also no significant dissimilarity in the house damage rate, as it was 62.44 per 1000 households in both regions. In the case of Cyclone Yaas (2021), the fatality rate was negligible at 0.19 per 100,000 in the Sundarban-safe zones and 0.20 per 100,000 in the unsecured zones. The house damage rate was 68.15 per 1000 in districts with protection and 71.58 per 1000 in districts without protection, indicating a slight change over recent years. Lastly, the rates of deaths and houses damaged were equivalent in the protected and unprotected areas during Cyclone Remal (2024), at 0.13 and 47.93 per 100,000 people and 1000 households.

Table 4: Cyclone-wise death rate and house damage rate for Sundarban-protected vs. unprotected districts

Year	Cyclone	Sundarban Protected Death Rate (per 100000)	Sundarban Unprotected Death Rate (per 100000)	House Damage (Sundarban Protected) (per 1000)	House Damage (Sundarban Unprotected) (per 1000)
2007	Sidr	113.1	249.41	2265.08	4995.04
2009	Aila	8.25	10.55	1306.37	1669.98
2019	Fani	2.04	1.91	48.45	45.23
2020	Amphan	1.72	1.54	62.44	62.44
2021	Yaas	0.19	0.2	68.15	71.58
2024	Remal	0.13	0.13	47.93	47.93

Data Sources: Bangladesh Bureau of Statistics (2001, 2011, & 2022), Bangladesh Meteorological Department

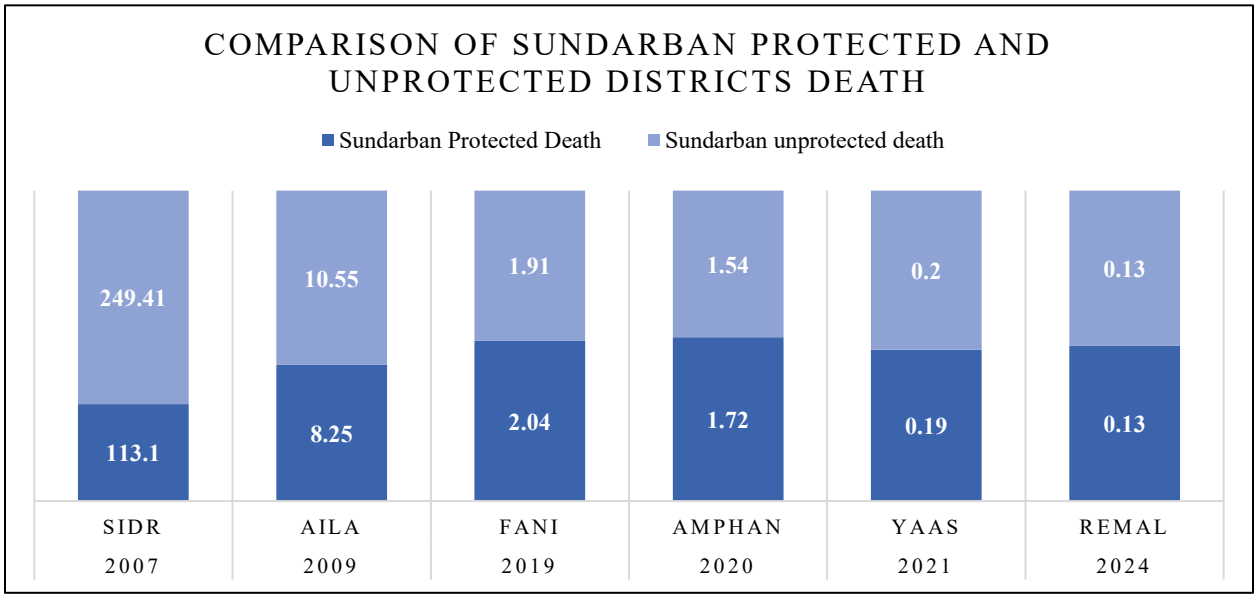


Fig. 5 Comparison of the Sundarban Protected and Unprotected districts' deaths

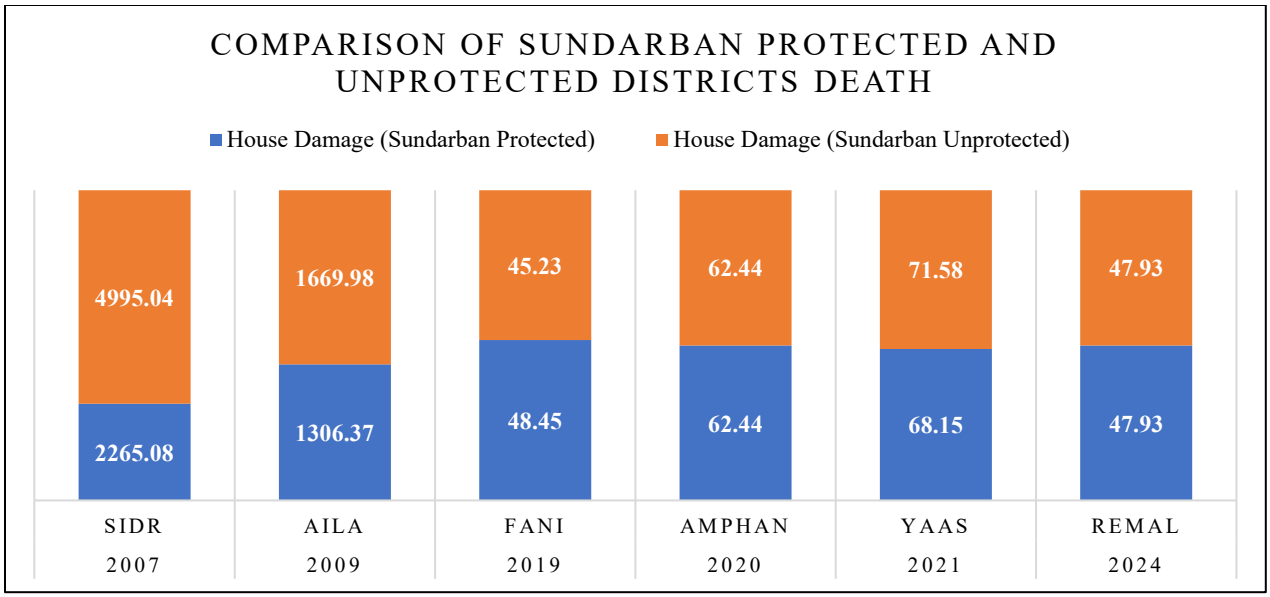


Fig. 6 Comparison of Sundarban Protected and Unprotected districts House Damage

4.5. Cyclone Track Mapping and Spatial Distribution of Affected Areas:

To illustrate the spatial distribution and frequency of cyclone landfalls in the Sundarbans area, cyclone tracks of Sidr (2007), Aila (2009), Fani (2019), Amphan (2020), Yaas (2021), and Remal (2024) were plotted using GIS. The cyclone track shapefiles have been obtained from the International Best Track Archive for Climate Stewardship (IBTrACS) dataset, available through NOAA data, which includes the geographic positions of cyclone centers taken at six-hour intervals. Each track was superimposed on the Sundarbans limit and the coastal districts surrounding this limit to determine the proximity to landfall and the direct effects on the forest and human settlements in the vicinity of the forest. A Kernel Density Estimation (KDE) analysis was conducted on the cyclone track points to identify areas with the highest exposure to cyclone impacts. The identified kernel density surface highlighted body regions of intense cyclone activities between 2007 and 2024. The values of higher density of the kernel were observed on the southwestern belt of coastal areas, especially in Khulna, Satkhira, Bagerhat, and Barguna districts, showing that these areas are most prone to constant exposure to cyclones. The spatial distribution and kernel density of cyclone tracks are illustrated in (**Fig. 7**), while (**Fig. 8**) shows the historical cyclone tracks affecting the Sundarbans region, the Sundarbans Protected Area is particularly vulnerable to these dense cyclone routes, which underscores the importance of this location as the

initial safeguard against storm surges and the effects of coastal winds. Additionally, the kernel density surface revealed secondary areas of vulnerability that extended into the inland region, which were geographically situated in areas previously identified as having high population density and housing damage, thereby highlighting the gradient of socio-environmental exposure between the coast and the interior regions.

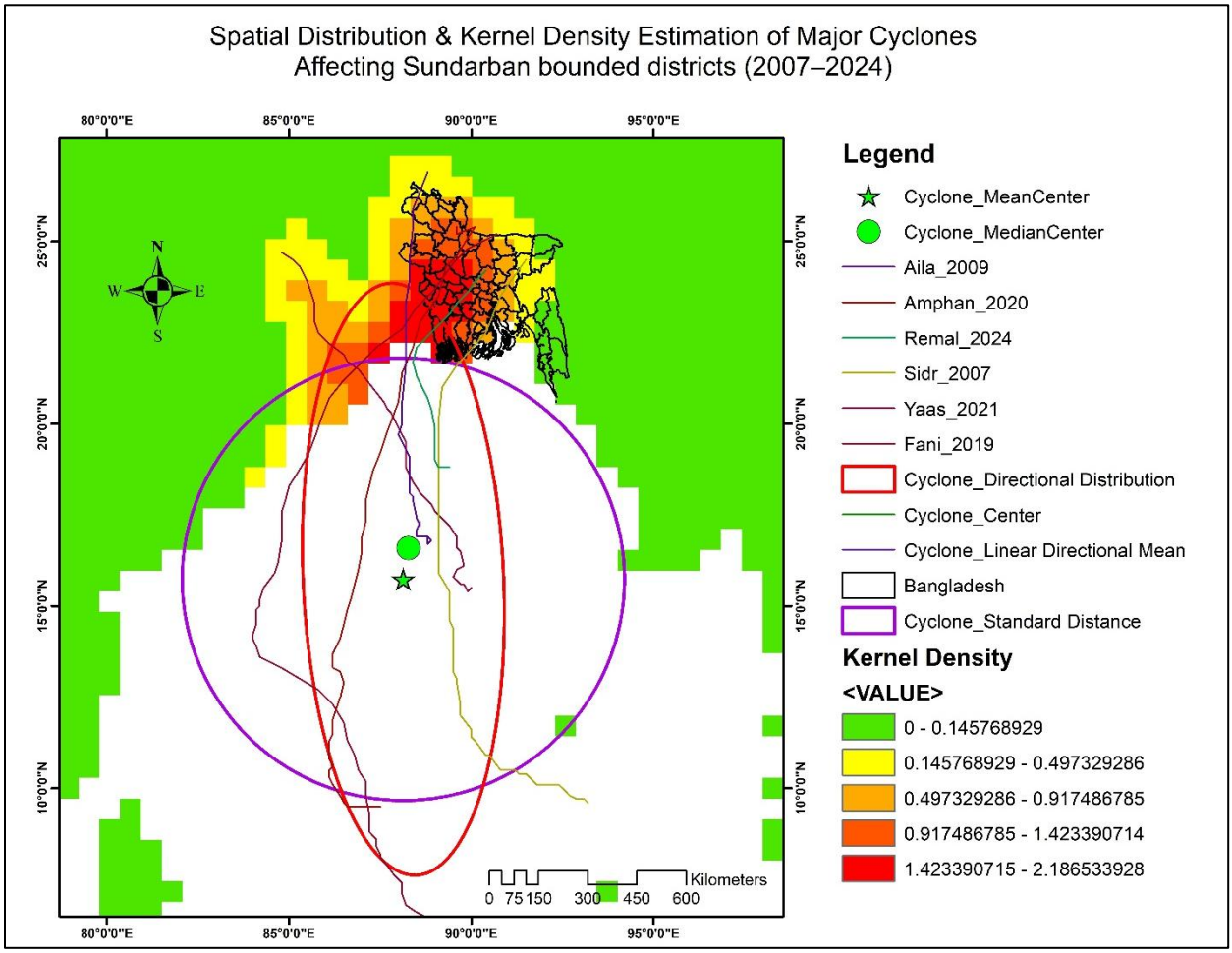
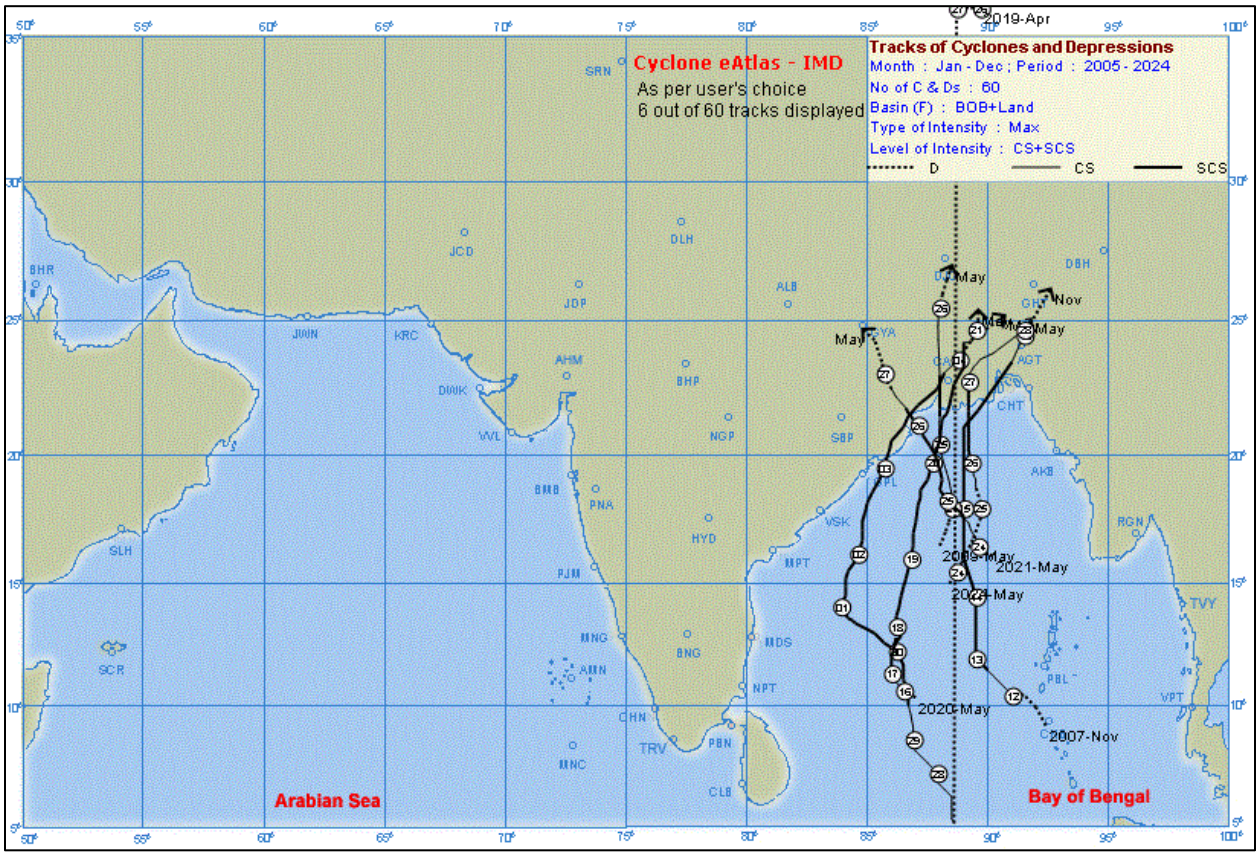


Fig. 7 Spatial Distribution & Kernel density estimation of major cyclones affecting Sundarban-bound districts



369 Source: eAtlas

370 **Fig. 8** Cyclone Tracks Map

371

372

373 **4.6. Statistical Relationships Between Vegetation and Cyclone Impact:**

374 A correlation analysis (Table 4) was conducted to determine the relationship between vegetation
375 cover and indicators of cyclone impact, such as the rate of mortality and the rate of house damage,
376 in both the Sundarban-guarded and non-guarded coastal areas.

377 Sparse vegetation is correlated with death rate (r = -0.139 in the same direction in protected and
378 unprotected areas) and house damage rate (r = -0.075 and -0.113), as well as the weak negative
379 correlation with surge height (r = -0.510) and the insignificant positive correlation with wind speed
380 (r = 0.072). Moderate vegetation has a weak negative correlation with death (r = -0.109 and -0.112)
381 and house damage rates (r = -0.021 and -0.038) and a moderate positive correlation with surge

height (r = 0.544) and a weak negative correlation with wind speed (r = -0.174). Dense vegetation exhibits weak positive correlations with death rates (r = 0.187 and 0.190) and house damage rates (r = 0.072 and 0.127), as well as positive correlations with surge height (r = 0.539) and wind speed (r = 0.191). Mean NDVI shows moderate negative correlations with death (r = -0.352 and -0.330) and house damage rates (r = -0.688 and -0.547), indicating less devastating events of a cyclone with more vigorous vegetation, and weak positive relations with the surge height (r = 0.311) and wind speed (r = 0.145). Mean EVI, though, has weak positive relationships with death (r = 0.102 and 0.078) and house damage rates (r = 0.557 and 0.358), and moderate negative relationships with surge height (r = -0.416) and wind speed (r = -0.652), indicating inconsistent relationships between vegetation enhancement and cyclone strength (Table 5).

Table 5:Correlation between Vegetation Indices and Cyclone Impact (Death and House Damage Rates)

	Sundarban Protected Area Death Rate	Sundarban Unprotected Area Death Rate	Sundarban Protected Area House Damage Rate	Sundarban Unprotected Area House Damage Rate	Surge Height (m)	Wind Speed (Km/h)
Sparse Vegetation	-0.139	-0.148	-0.075	-0.113	-0.51	0.072
Moderate Vegetation	-0.109	-0.112	-0.021	-0.038	0.544	-0.174
Dense Vegetation	0.187	0.190	0.072	0.127	0.539	0.191
Mean NDVI	-0.352	-0.330	-0.688	-0.547	0.311	0.145
Mean EVI	0.102	0.078	0.557	0.358	-0.416	-0.652

4.7. Regression Analysis of NDVI,EVI, and Cyclone Impact Variables in Sundarban Protected and Unprotected Areas:

Regression analysis revealed a significant and similar relationship between vegetation indices (NDVI and EVI) and cyclone-induced effects in both the Sundarban protected and unprotected areas. In all models, a statistically significant negative association was found between the mean EVI and the rates of death and house damage. In the case of the protected areas, EVI was strongly negatively correlated with the death rate ($\beta = -0.888$, $p = 0.018$) and the house damage rate ($\beta = -0.962$, $p = 0.002$). Likewise, the meanings of EVI were found to be significantly and negatively correlated with both the death rate ($\beta = -0.875$, $p = 0.022$) and house damage rate ($\beta = -0.954$, $p = 0.003$) in unprotected areas. In the Sundarban shielded area, Mean NDVI was negatively correlated with the death rate ($\beta = -0.352$, $p = 0.494$) and house damage rate ($\beta = -0.688$, $p = 0.131$), which meant that the vegetation density was slightly associated with lower mortality and reconstruction of houses caused by a cyclone, albeit not at a statistically significant level. The relationship in the unprotected coastal area followed a similar pattern, with NDVI being negatively correlated with the death rate ($\beta = -0.330$, $p = 0.524$) and the house damage rate ($\beta = -0.547$, $p = 0.261$) (Table 6). These findings suggest that, although NDVI is generally associated with greener vegetation and lower cyclone impact, it is not a strong predictor of cyclone impact compared to EVI and the relationships between EVI. The relationship between EVI and death rate and house damage rate is shown in (**Fig. 9)**, while the relationship between NDVI and death rate and house damage is presented in (**Fig. 10)**.

Table 6: Summary of Regression Results for Vegetation Indices and Cyclone Impacts in the Sundarbans (2007–2024)

Dependent Variable	Independent Variable	Unstandardized Coefficient (B)	Std. Error	Standardized Coefficient (β)	t-value	Sig. (p)	VIF
Sundarban Protected Death Rate	Mean NDVI	-754.792	835.451	-0.352	-0.753	0.494	1.000
	Mean EVI	-1159.123	300.615	-0.888	-3.856	0.018	1.000

Sundarban Unprotected Death Rate	Mean NDVI	-1571.658	2251.215	-0.330	-0.698	0.524	1.000
	Mean EVI	-2542.547	703.285	-0.875	-3.615	0.022	1.000
Sundarban Protected House Damage Rate	Mean NDVI	-30718.731	16196.950	-0.688	-1.897	0.131	1.000
	Mean EVI	-26160.041	3726.832	-0.962	-7.019	0.002	1.000
Sundarban Unprotected House Damage Rate	Mean NDVI	-51619.569	39457.778	-0.547	-1.308	0.261	1.000
	Mean EVI	-54830.684	8585.591	-0.954	-6.386	0.003	1.000

421

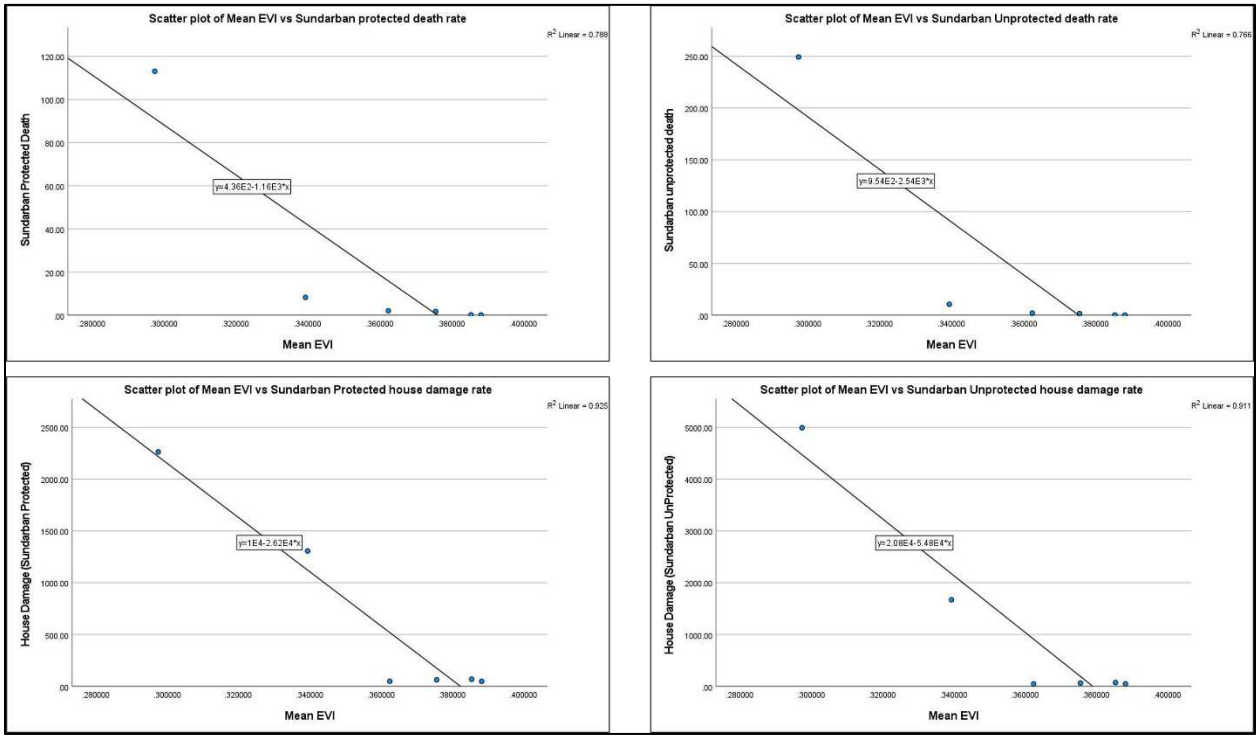


Fig. 1 Scatter Plot of EVI vs Sundarban Protected and Unprotected Death rate and House Damage

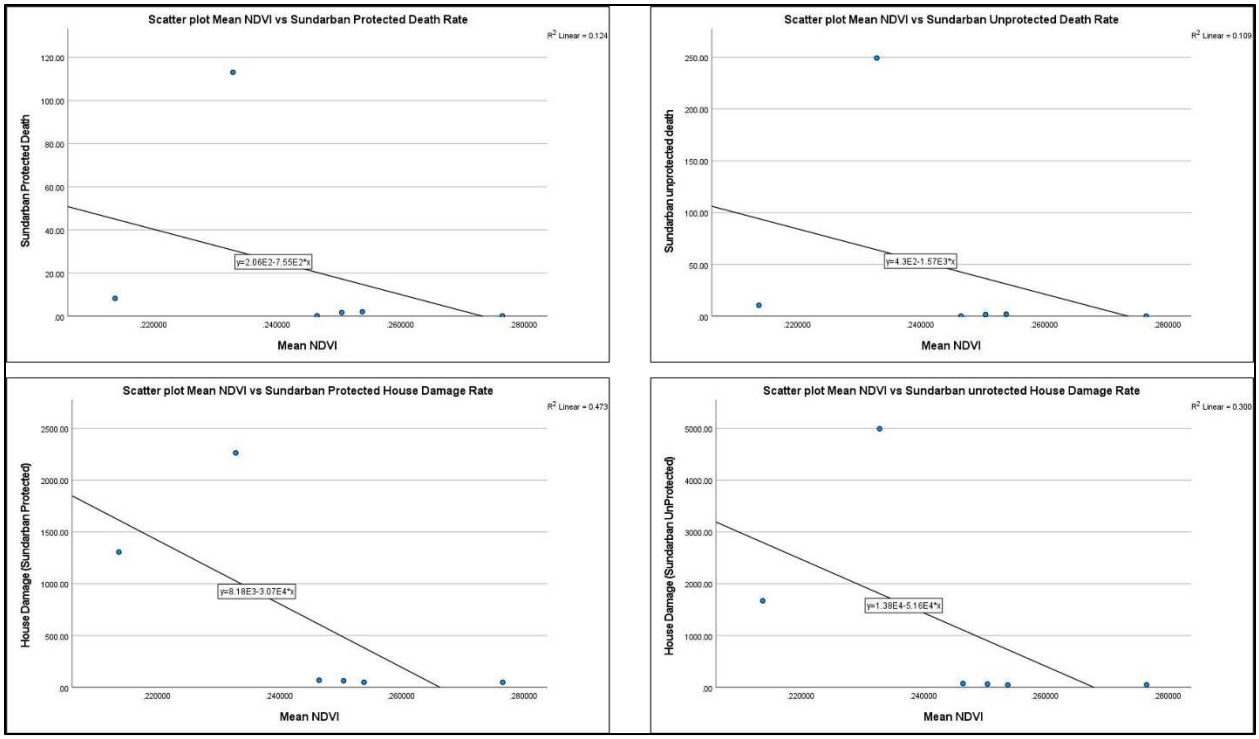


Fig. 10 Scatter Plot of NDVI vs Sundarban Protected and Unprotected Death rate and House Damage

4.8. Accuracy Assessment of Vegetation Indices:

The assessment of the accuracy of NDVI and EVI classifications for 2007, 2009, 2019, 2020, 2021, and 2024 demonstrated high performance in all years. In the case of NDVI, the overall accuracies in 2007, 2009, 2019, 2020, 2021, and 2024 were 88.7% (Kappa = 0.84), 89.1% (Kappa = 0.85), 91.3% (Kappa = 0.89), 90.5% (Kappa = 0.88), 89.8% (Kappa = 0.86), and 92.3% (Kappa = 0.91), respectively. Equally, EVI classifications had a slightly higher accuracy of 89.5%(Kappa = 0.86) in 2007, 90.2% (Kappa = 0.87) in 2009, 92.1% (Kappa = 0.90) in 2019, 91.4% (Kappa = 0.89) in 2020, 90.7% (Kappa = 0.88) in 2021, and 93.4% (Kappa = 0.92) in 2024 (Table 7). The regular significant overall accuracies (exceeding 88%) and Kappa values (exceeding 0.84) demonstrate a high level of agreement between the ground truth data and the classified outputs.

Table 7: Accuracy Assessment of Vegetation Indices

Year	Index	Overall Accuracy (%)	Kappa Coefficient
2007	NDVI	88.7	0.84
	EVI	89.5	0.86
2009	NDVI	89.1	0.85
	EVI	90.2	0.87
2019	NDVI	91.3	0.89
	EVI	92.1	0.90
2020	NDVI	90.5	0.88
	EVI	91.4	0.89
2021	NDVI	89.8	0.86
	EVI	90.7	0.88
2024	NDVI	92.3	0.91
	EVI	93.4	0.92

5. Discussion

The present study examined how vegetation health, as measured by the Normalized Difference Vegetation Index (NDVI) and Enhanced Vegetation Index (EVI), affects cyclone-related deaths and house damage in protected and non-protected areas of the Sundarban between 2007 and 2024. It is found that vegetation indices and cyclone effects show a negative correlation, providing conclusive evidence that a dense, healthy layer of mangrove cover significantly reduces disaster vulnerability along the Bangladesh coastline.

Regression analysis showed that the Mean EVI was significantly negatively correlated with the death rate and the house damage rate in the protected and unprotected areas. There was a negative relationship between EVI and cyclone deaths ($b = -0.888$, $p = 0.018$) and house damage ($b = -$

0.962, p = 0.002) in Sundarban protected areas, suggesting that greater vegetation density reduces the effects of cyclones by buffering winds and storm waves. On the same note, EVI in unprotected regions also exhibited significant negative correlation with the death rate (b = -0.875, p = 0.022) and house damage (b = -0.954, p = 0.003). These results support previous research asserting that mangroves have the potential to attenuate waves by more than 66 per cent within 100 m of forest cover and to diminish surges and wind power extending to inland settlements substantially (Mazda et al., 2006; McIvor et al., 2012; Narayan et al., 2017).

The weaker performance of NDVI compared to EVI is consistent with previous studies that have indicated that NDVI tends to oversaturate in dense vegetation habitats, leading to an underestimation of canopy variation in mangrove forests (Huete et al., 2002). However, NDVI continued to show a negative correlation with death and damage rates, indicating that vegetation greenness in an area tends to experience fewer losses during cyclones. This higher sensitivity of EVI to high-biomass environments therefore provides stronger evidence of mangrove health and cyclone mitigation capacity.

The detection of NDVI changes from 2007 to 2024 demonstrated a very slight, though significant, shift in vegetation structure in the Bangladeshi Sundarbans. The amount of dense vegetation decreased slightly (-1.04%), sparse vegetation decreased sharply (-47.9%), and water-covered areas increased by 127%. These changes in deforestation can be caused by cyclones, erosion, tides, salinity intrusion, and frequent extreme events, including Sidr (2007), Aila (2009), and Amphan (2020). Similar effects and outcomes were previously reported: in the season of large cyclones, the mortality rate of trees can be up to 10-15% of all trees in very severe areas, and recovery needs a long time (Iftekhar and Saenger, 2008; Hasan et al., 2020; Samanta et al., 2021). The recovery of vegetation in 2024 was moderate, indicating that mangrove ecosystems are inherently resilient through natural regeneration, sediment accretion, and species adaptation (Alongi, 2015; Kanjin & Alam, 2024).

An interesting fact is that death tolls are occasionally higher in Sundarban protected areas than in unprotected areas during previous cyclones (such as Sidr 2007 and Aila 2009). However, the damage to houses was minimal. The geographical exposure can be attributed to this paradox: most of the covered districts (Khulna, Satkhira, Bagerhat) lie adjacent to cyclone landfall zones, where the force of surges and winds is concentrated first. In the meantime, better forest buffers and

amenities in inner unprotected regions are likely to have minimised death. However, over time, the mortality rate across all zones reduced significantly because the early warning system was reinforced, cyclone shelters were increased, and disaster preparedness was improved (Haque et al., 2012; Paul, 2014).

They were seven large cyclones, including: Sidr (2007), Aila (2009), Fani (2019), Amphan (2020), Yaas (2021), and Remal (2024), all of which were intentionally chosen. These incidents were the worst and the spatially vast tropical cyclones that hit the Bangladeshi Sundarbans throughout the research area, both pre- and post-disaster management periods. Sidr and Aila have been selected as high-intensity impact baselines without large-scale adaptation intervention and Fani, Amphan, Yaas, and Remal represent the intensifying and shifting nature of present-day cyclones in new climatic conditions and enhanced mitigation strategies. They collectively offer a timeframe for assessing changes in vegetation cover and management, and how vulnerability has been adjusted over the almost 20 years of exposure to tropical cyclones. These were also selected because they provide consistent data on human deaths and housing damage, and because the landfalls or tracks of these cyclones impacted both kinds of districts, allowing comparisons of the protective effects of the Sundarbans over time.

Finally, the statistical and spatial outcomes are consistent in showing that vegetation health, especially mangrove density and canopy vitality, is a very important factor in reducing the impact of cyclones. The significant negative regressions between EVI and the two variables, mortality and damage, support the biophysical ability of mangroves to absorb storm energy and protect populations on the inland land. This underscores a growing body of opinion on the fact that mangrove conservation and growth are among the most affordable, as well as sustainable solutions to climate adaptation in deltaic Bangladesh (Das & Vincent, 2009; Barbier, 2016; Narayan et al., 2017).

There are various limitations to this study. To start with, the sample size (six cyclone events) is not very massive and as such, it limits the statistical power and it is likely to produce non-significant in certain NDVI models. Second, the damage and death rates using district-level aggregated data can conceal the intra-district heterogeneity; more accurate information could be provided by finer-scale census or household-level. Third, although EVI and NDVI are good vegetation proxies, they fail to present structural variables such as tree height, tree biomass and root integrity, which also

play vital roles in the ability of mangroves to overcome wind and surge forces. Future studies should include LiDAR or UAV-based metrics of structural because these would enhance mechanistic knowledge. Also, cyclone path/surge modeling (integrating EVI change maps with kernel density of cyclone paths or hydrodynamic surge models) may be useful to identify areas of repetitive vulnerability, and help prioritize locations of restoration locations. Socio-economic, land-use change, and hydrological drivers (upstream sediment supply) controlling the mangrove dynamics should also be studied in the future. The empirical evidence presented in this paper enhances the argument in favor of the maintenance and rehabilitation of the mangrove cover as a low-cost nature-based measure of coastal protection. Having a healthy mangrove buffer (in the enclosed reserves, as well as in the fringe areas) will go a long way in minimizing loss of lives and property in case of cyclones. The policy makers must give focus on restoration of forests in areas where vegetation degradation or frequent exposure is identified through the use of change detecting maps. In addition, vegetation health monitoring (through EVI) should be incorporated in the disaster risk reduction framework, which may be beneficial in terms of the forecasting, zoning, and early warning measures. The ecosystem in the Sundarbans is in a state of constant tension between ecology and human response and adaptation, which implies that constant monitoring, adaptive management, and community involvement in the conservation and restoration activities are necessary.

6. Conclusion:

This research paper is highlighted the importance of mangrove vegetation in arresting the effects of cyclones in the Sundarbans and other coastal areas in Bangladesh. The study of seven large cyclones in 2007 to 2024 demonstrated that the density of vegetation increased the probability of reduced death and house destruction, which confirmed the protective effect of mangroves against the intense winds and storm surge. Despite noticing a marginal decrease in the dense vegetation cover in the period between 2007 and 2024, the Sundarbans are known to be highly resilient and able to recover. The declining pattern in the number of deaths due to cyclones over the years is an indicator that shows the synergy between the mangrove cover, the enhancement of the early warning systems and the community preparedness. On the whole, the results point out the fact that the vegetation cover (in and outside of the shielded Sundarbans) must be healthy to reduce the

losses in the case of a cyclone. Enhancing mangrove recovery and greenbelt zones should also be considered as the primary measures to improve the resilience of the coast and decrease the risk of disasters in Bangladesh.

References:

- Ali, Y., Roy, S. K., Rahman, M., & Hossain, M. (2025). Quantifying forest stocking changes in Sundarbans mangrove between 2000 and 2023: TCH, AGB, and carbon stock shifts. *Forest Ecology and Management*, 566, 122123. https://doi.org/10.1016/j.foreco.2024.122123
- Arif, M. S. I., Mamun, M. M. A., Hasan, M. M., Ahmed, B., & Dewan, A. (2023). Cyclone exposure mapping in coastal Bangladesh: A case of Taltali Upazila. *PLoS ONE, 18*(11), e0293465. https://doi.org/10.1371/journal.pone.0293465
- Hossain, K. A., Akhter, S., Rahman, M. R., & Habiba, U. (2024). Land cover change across 45 years in the world's largest mangrove forest: Sundarbans, Bangladesh. *Journal of Coastal Conservation, 28*(1), 12. https://doi.org/10.1007/s11852-023-00958-7
- Islam, M. A., Das, B. C., & Ali, E. (2024). Perception, problems, and risks to climate change adaptation in southwestern coastal Bangladesh adjacent to Sundarbans. *Environmental Systems Research, 13*(1), 7. https://doi.org/10.1186/s40068-024-00345-4
- Mamun, M. M. A., Ahmed, B., Dewan, A., & Islam, M. M. (2025). Cyclone surge inundation susceptibility assessment in Bangladesh using AHP and fuzzy logic. *Frontiers in Earth Science, 13*, 1554864. https://doi.org/10.3389/feart.2025.1554864
- Mancheño, A. G., Jafino, B. A., van Wesenbeeck, B. K., Haque, A., & van Dongeren, A. (2025). Nature meets infrastructure: The role of mangroves in strengthening Bangladesh's coastal flood defenses. *Sustainability, 17*(4), 1567. https://doi.org/10.3390/su17041567
- Roy, S. K., Rahman, M., & Hossain, M. (2025). Evaluating mangrove forest dynamics and fragmentation in the Sundarbans, Bangladesh from 2017 to 2023 using Sentinel-2 imagery. *Environmental Research Letters, 20*(3), 035004. https://doi.org/10.1088/1748-9326/ad95a0
- Siddique, M. R. H., Iftekhar, M. S., Islam, K. M. A., & Datta, D. (2024). Evaluating co-management practices in the Sundarbans mangrove: Challenges, governance, and institutional efficacy. *Ecology and Society, 29*(2), 8. https://doi.org/10.5751/ES-14887-290208
- Zhang, Z., Islam, M. M., Zeng, T., & Liu, Y. (2023). Monitoring of 35-year mangrove wetland change in the Sundarbans using Landsat imagery (1988–2022). *Remote Sensing, 15*(3), 625. https://doi.org/10.3390/rs15030625

- Bangladesh Bureau of Statistics (BBS). (2022). *Population and housing census 2022: Preliminary report*. Dhaka: Bangladesh Bureau of Statistics, Government of Bangladesh.
- Congalton, R. G., & Green, K. (2009). *Assessing the accuracy of remotely sensed data: Principles and practices* (2nd ed.). Boca Raton, FL: CRC Press.
- Das, S., & Vincent, J. R. (2009). Mangroves protected villages and reduced death toll during Indian super cyclone. *Proceedings of the National Academy of Sciences, 106*(18), 7357–7360. https://doi.org/10.1073/pnas.0810440106
- Giri, C., Long, J., Abbas, S., Murali, R. M., Qamer, F. M., Pengra, B., & Thau, D. (2015). Distribution and dynamics of mangrove forests of South Asia. *Journal of Environmental Management, 148*, 101–111. https://doi.org/10.1016/j.jenvman.2014.01.020
- Iftekhar, M. S., & Saenger, P. (2008). Vegetation dynamics in the Bangladesh Sundarbans mangroves: A review of forest inventories. *Wetlands Ecology and Management, 16*(4), 291–312. https://doi.org/10.1007/s11273-007-9063-5
- Paul, B. K., & Routray, J. K. (2011). Household response to cyclone and induced surge in coastal Bangladesh: Coping strategies and explanatory variables. *Natural Hazards, 57*(2), 477–499. https://doi.org/10.1007/s11069-010-9625-4
- Shahid, S., & Behrawan, H. (2008). Drought risk assessment in the western part of Bangladesh. *Natural Hazards, 46*(3), 391–413. https://doi.org/10.1007/s11069-007-9191-5
- Chavez, P. S. (1996). Image-based atmospheric corrections—Revisited and improved. *Photogrammetric Engineering and Remote Sensing, 62*(9), 1025–1036.
- Zhu, Z., & Woodcock, C. E. (2012). Object-based cloud and cloud shadow detection in Landsat imagery. *Remote Sensing of Environment, 118*, 83–94. https://doi.org/10.1016/j.rse.2011.10.028
- Giri, C., Long, J., Abbas, S., Murali, R. M., Qamer, F. M., Pengra, B., & Thau, D. (2015). Distribution and dynamics of mangrove forests of South Asia. *Journal of Environmental Management, 148*, 101–111. https://doi.org/10.1016/j.jenvman.2014.01.020
- Huete, A., Didan, K., Miura, T., Rodriguez, E. P., Gao, X., & Ferreira, L. G. (2002). Overview of the radiometric and biophysical performance of the MODIS vegetation indices. *Remote Sensing of Environment, 83*(1–2), 195–213. https://doi.org/10.1016/S0034-4257(02)00096-2

- Rouse, J. W., Haas, R. H., Schell, J. A., & Deering, D. W. (1974). Monitoring vegetation systems in the Great Plains with ERTS. In *Proceedings of the Third Earth Resources Technology Satellite-1 Symposium* (Vol. 1, pp. 309–317). NASA SP-351.
- Foody, G. M. (2002). Status of land cover classification accuracy assessment. *Remote Sensing of Environment, 80*(1), 185–201. https://doi.org/10.1016/S0034-4257(01)00295-4
- Alongi, D. M. (2015). *The impact of climate change on mangrove forests*. Current Climate Change Reports, 1(1), 30–39. https://doi.org/10.1007/s40641-015-0002-x
- Barbier, E. B. (2016). The protective service of mangrove ecosystems: A review of valuation methods. *Marine Pollution Bulletin, 109*(2), 676–681. https://doi.org/10.1016/j.marpolbul.2016.01.033
- Das, S., & Vincent, J. R. (2009). Mangroves protected villages and reduced death toll during Indian super cyclone. *Proceedings of the National Academy of Sciences, 106*(18), 7357–7360. https://doi.org/10.1073/pnas.0810440106
- Haque, U., Hashizume, M., Kolivras, K. N., Overgaard, H. J., Das, B., & Yamamoto, T. (2012). Reduced death rates from cyclones in Bangladesh: What more needs to be done? *Bulletin of the World Health Organization, 90*(2), 150–156. https://doi.org/10.2471/BLT.11.088302
- Hasan, M. S., Mandal, T., & Hosaka, T. (2020). Assessing cyclone disturbances (1988–2016) in the Sundarbans mangrove forests using Landsat and Google Earth Engine. *Natural Hazards, 102*(1), 133–150. https://doi.org/10.1007/s11069-020-03914-z
- Huete, A. R., Didan, K., Miura, T., Rodriguez, E. P., Gao, X., & Ferreira, L. G. (2002). Overview of the radiometric and biophysical performance of the MODIS vegetation indices. *Remote Sensing of Environment, 83*(1–2), 195–213. https://doi.org/10.1016/S0034-4257(02)00096-2
- Iftekhar, M. S., & Saenger, P. (2008). Vegetation dynamics in the Bangladesh Sundarbans mangroves: A review of forest inventories. *Wetlands Ecology and Management, 16*(4), 291–312. https://doi.org/10.1007/s11273-007-9063-5
- Kanjin, K., & Alam, B. M. (2024). Assessing changes in land cover, NDVI, and land surface temperature in the Sundarbans mangrove forest in Bangladesh and India: A GIS and remote sensing approach. *Remote Sensing Applications: Society and Environment, 34*, 101289. https://doi.org/10.1016/j.rsase.2024.101289

- Mazda, Y., Magi, M., Kogo, M., & Hong, P. N. (2006). Wave reduction in a mangrove forest dominated by Sonneratia sp. *Wetlands Ecology and Management, 14*(4), 365–378. https://doi.org/10.1007/s11273-005-5388-0
- McIvor, A. L., Spencer, T., Möller, I., & Spalding, M. (2012). *Storm surge reduction by mangroves*. The Nature Conservancy & Wetlands International.
- Narayan, S., Beck, M. W., Reguero, B. G., Losada, I. J., van Wesenbeeck, B., Pontee, N., Sanchirico, J. N., Ingram, J. C., & Burke, L. (2017). The effectiveness, costs, and coastal protection benefits of natural and nature-based defenses. *PLOS ONE, 11*(5), e0154735. https://doi.org/10.1371/journal.pone.0154735
- Paul, B. K. (2014). Why relatively fewer people died? The case of Bangladesh's Cyclone Sidr. *Natural Hazards, 68*(2), 685–703. https://doi.org/10.1007/s11069-013-0630-2
- Samanta, S., Hazra, S., Mondal, P. P., Chanda, A., Giri, S., French, J. R., & Nicholls, R. J. (2021). Assessment and attribution of mangrove forest changes in the Indian Sundarbans from 2000 to 2020. *Remote Sensing, 13*(24), 4957. https://doi.org/10.3390/rs13244957

Declaration of Statements:

Ethical Approval

This study did not involve human participants, animals, or field experiments requiring ethical

approval. All data used (satellite imagery, cyclone track datasets, and secondary statistics) are publicly available and obtained from open-access sources that permit academic use.

Consent to Participate

Not applicable, as the study did not involve human subjects.

Consent for Publication

All authors give full consent for the publication of this manuscript in *Environmental Monitoring and Assessment*

Competing Interests

The authors declare that they have no known competing financial interests or personal relationships that could have appeared to influence the work reported in this paper.

Funding

This research did not receive any specific grant from funding agencies in the public, commercial, or not-for-profit sectors.

Authors Contributions

- **Kazi Sajirul Kadir Apon**: Conceptualization, data collection, satellite image processing, analysis, writing original draft, GIS mapping.
- **Tania Sultana**: Literature review, data verification, writing review & editing, formatting.

All authors have read and approved the final manuscript.

Availability of Data and Materials

All datasets analyzed in this study are publicly accessible.

- Landsat imagery: USGS Earth Explorer
- Cyclone track: NOAA IBTrACS
- Disaster statistics: BBS & EM-DAT

  Data processed during the study can be provided by the corresponding author upon reasonable request.

Clinical trial

Clinical trial number: not applicable.